

Double photoionization of helium including quadrupole radiation effects

J A Ludlow¹, J Colgan², Teck-Ghee Lee¹, M S Pindzola¹ and F Robicheaux¹

¹ Department of Physics, Auburn University, Auburn, AL 36849, USA

² Theoretical Division, Los Alamos National Laboratory, Los Alamos, NM 87545, USA

Received 24 July 2009, in final form 7 October 2009

Published 5 November 2009

Online at stacks.iop.org/JPhysB/42/225204

Abstract

Non-perturbative time-dependent close-coupling calculations are carried out for the double photoionization of helium including both dipole and quadrupole radiation effects. At a photon energy of 800 eV, accessible at current synchrotron light sources, the quadrupole interaction contributes around 6% to the total integral double photoionization cross section. The pure quadrupole single energy differential cross section shows a local maximum at equal energy sharing, as opposed to the minimum found in the pure dipole single energy differential cross section. The sum of the pure dipole and pure quadrupole single energy differentials is insensitive to non-dipole effects at 800 eV. However, the triple differential cross section at equal energy sharing of the two ejected electrons shows strong non-dipole effects due to the quadrupole interaction that may be experimentally observable.

(Some figures in this article are in colour only in the electronic version)

1. Introduction

The validity of the dipole approximation in calculations of double photoionization rests on the assumption that higher order multipoles can be neglected. Generally, for low photon energies this is reasonable, however, the dipole approximation is expected to break down at higher photon energies. Double photoionization of helium has been the subject of numerous investigations, both experimental [1–3] and theoretical [4–6] with good agreement found between theory and experiment at low photon energies.

The single energy differential cross section due to the dipole interaction is now well understood. At an excess photon energy of 20 eV, the single energy differential cross section is almost flat [7]. This is due to a ‘knock out’ mechanism that dominates at low photon energies in which the electron that absorbs the photon ‘knocks out’ the other electron as it is being ionized. This is referred to as the two-step-one (TS1) mechanism in the double ionization of atoms by photons or electrons. This process does not depend strongly on the energy sharing between the electrons, leading to a flat single energy differential cross section. For a photon energy of 529 eV the single energy differential cross section has been shown to be ‘U’ shaped, with one ejected electron taking almost all the excess energy [8]. This has been explained via the ‘shake-off’

mechanism that dominates the dipole cross section at higher energies. This process involves one electron absorbing the photon and being ionized. The sudden change in the atomic potential caused by the ejection of the first electron causes the second electron to have a probability of relaxing to a continuum state of He⁺, i.e. it is ‘shaken off’. This process will typically produce one slow and one fast electron, so explaining the ‘U’ shape observed in the single energy differential cross section.

The influence of non-dipole effects has been investigated within the framework of lowest-order perturbation theory (LOPT) [9, 10], with a non-dipole forward–backward asymmetry predicted in the triple differential cross section at an excess energy of 450 eV. The importance of accounting for non-dipole effects was confirmed by subsequent non-perturbative convergent close-coupling calculations [11, 12]. At higher photon energies the single energy differential cross section has been predicted to show more structure with a ‘W’ shape developing due to the quadrupole interaction [13, 14]. This proposed structure can be understood as arising due to a mechanism whereby a pair of electrons could absorb a single photon in the quadrupole (or higher multipole) approximation such that the nucleus would hardly recoil. To see how this mechanism arises, examine the dipole operator

for two electrons through the quadrupole term for light linearly polarized in the z -direction and travelling in the x -direction:

$$D = p_{z_1} e^{ikx_1} + p_{z_2} e^{ikx_2} \simeq p_{z_1} + p_{z_2} + ik(p_{z_1}x_1 + p_{z_2}x_2), \quad (1)$$

where k is the wave number of the photon and p_z is the z component of the momentum operator. If the electron coordinates are written in centre-of-mass form ($x_- = x_2 - x_1$, $x_+ = (x_2 + x_1)/2$) and $p_{z_+} = p_{z_1} + p_{z_2}$, $p_{z_-} = (p_{z_2} - p_{z_1})/2$, then the transition operator can be written as

$$D \simeq p_{z_+} + ik(p_{z_+}x_+ + p_{z_-}x_-). \quad (2)$$

The part of the operator that depends on the '+' coordinate gives substantial nuclear recoil because this coordinate is relative to the nucleus, thus the electron momentum is opposite to that of the nucleus. But note that at the quadrupole level, there is a term in the operator that directly acts on the relative coordinate ($p_{z_-}x_-$). This term allows a transition where the electron–electron relative coordinate absorbs the energy and momentum of the photon. Since the nucleus is not involved in the transition, it only recoils through the post collision interaction of the outgoing electron with the nuclear charge. Since the electrons are travelling in opposite directions with nearly equal speed, this interaction will be suppressed. This leads to a maximum in the single energy differential cross section at equal energy sharing.

Here we test this prediction by carrying out an *ab initio* calculation using the time-dependent close-coupling method (TDCC) [15] of the double photoionization of helium including the quadrupole interaction and calculate the total integral cross section, the single energy differential cross section and the triple differential cross section. In the following section, we discuss the extension to the theory that is needed to incorporate the quadrupole interaction, and then present results at a photon energy of 800 eV. This energy should be within the range of existing synchrotron sources and is accessible to *ab initio* theory. Unless otherwise stated we use atomic units throughout.

2. Theory

For the double photoionization of an atom with two active electrons, the time-dependent Schrödinger equation in the weak field limit is given by

$$i \frac{\partial \Psi(\vec{r}_1, \vec{r}_2, t)}{\partial t} = H_{\text{atom}} \Psi(\vec{r}_1, \vec{r}_2, t) + H_{\text{rad}} \Psi_0(\vec{r}_1, \vec{r}_2) e^{-iE_0 t}, \quad (3)$$

where

$$H_{\text{atom}} = \sum_i^2 \left(-\frac{1}{2} \nabla_i^2 + V(r_i) \right) + \frac{1}{|\vec{r}_1 - \vec{r}_2|} \quad (4)$$

and $V(r) = -2/r$ for the helium atom. For a linearly polarized radiation field in the length gauge:

$$H_{\text{rad}} = \left(\frac{\omega}{c} \right)^{n-1} E(t) \cos \omega t \sum_i^2 r_i^n C^n(\hat{r}_i), \quad (5)$$

where ω is the radiation field frequency, c is the speed of light, $E(t)$ is the radiation field amplitude, $C^n(\hat{r}) = \sqrt{\frac{4\pi}{2n+1}} Y_{n0}(\hat{r})$ is a spherical tensor, $Y_{nm}(\hat{r})$ is a spherical harmonic, $n = 1$ for dipole interactions and $n = 2$ for quadrupole interactions. The wavefunction, $\Psi_0(\vec{r}_1, \vec{r}_2)$, and energy, E_0 , for the ground state of an atom with two active electrons is obtained by relaxation of the time-dependent Schrödinger equation in imaginary time ($\tau = it$):

$$-\frac{\partial \Psi_0(\vec{r}_1, \vec{r}_2, \tau)}{\partial \tau} = H_{\text{atom}} \Psi_0(\vec{r}_1, \vec{r}_2, \tau). \quad (6)$$

Expanding $\Psi(\vec{r}_1, \vec{r}_2, t)$ and $\Psi_0(\vec{r}_1, \vec{r}_2, \tau)$ in coupled spherical harmonics and substitution into equations (3) and (6) yields the time-dependent close-coupled equations [7]:

$$i \frac{\partial P_{l_1 l_2}^{LS}(r_1, r_2, t)}{\partial t} = T_{l_1 l_2}(r_1, r_2) P_{l_1 l_2}^{LS}(r_1, r_2, t) + \sum_{l'_1, l'_2} V_{l_1 l_2, l'_1 l'_2}^L(r_1, r_2) P_{l'_1 l'_2}^{LS}(r_1, r_2, t) + \sum_{l'_1, l'_2} W_{l_1 l_2, l'_1 l'_2}^{LL'}(r_1, r_2, t) \bar{P}_{l'_1 l'_2}^{LS}(r_1, r_2, \tau \rightarrow \infty) e^{-iE_0 t} \quad (7)$$

and

$$-\frac{\partial \bar{P}_{l_1 l_2}^{LS}(r_1, r_2, \tau)}{\partial \tau} = T_{l_1 l_2}(r_1, r_2) \bar{P}_{l_1 l_2}^{LS}(r_1, r_2, \tau) + \sum_{l'_1, l'_2} V_{l_1 l_2, l'_1 l'_2}^L(r_1, r_2) \bar{P}_{l'_1 l'_2}^{LS}(r_1, r_2, \tau). \quad (8)$$

The one-body operator is given by

$$T_{l_1 l_2}(r_1, r_2) = \sum_i^2 \left(-\frac{1}{2} \frac{\partial^2}{\partial r_i^2} + \frac{l_i(l_i + 1)}{2r_i^2} + V(r_i) \right) \quad (9)$$

and the two-body Coulomb operator is given by

$$V_{l_1 l_2, l'_1 l'_2}^L(r_1, r_2) = (-1)^{L+l_2+l'_2} \sqrt{(2l_1+1)(2l'_1+1)(2l_2+1)(2l'_2+1)} \times \sum_{\lambda} \frac{r_{<}^{\lambda}}{r_{>}^{\lambda+1}} \begin{pmatrix} l_1 & \lambda & l'_1 \\ 0 & 0 & 0 \end{pmatrix} \begin{pmatrix} l_2 & \lambda & l'_2 \\ 0 & 0 & 0 \end{pmatrix} \begin{Bmatrix} L & l'_2 & l'_1 \\ \lambda & l_1 & l_2 \end{Bmatrix}, \quad (10)$$

where $r_{<} = \min(r_1, r_2)$, $r_{>} = \max(r_1, r_2)$, and standard $3j$ and $6j$ symbols are used. The one-body radiation field operator is given by

$$W_{l_1 l_2, l'_1 l'_2}^{LL'}(r_1, r_2, t) = \left(\frac{\omega}{c} \right)^{n-1} E(t) \cos \omega t \sqrt{(2L+1)(2L'+1)} \times \left((-1)^{l_2+L+L'+n} \delta_{l_2, l'_2} \sqrt{(2l_1+1)(2l'_1+1)} \right. \\ \times r_1^n \begin{pmatrix} l_1 & n & l'_1 \\ 0 & 0 & 0 \end{pmatrix} \begin{pmatrix} L & n & L' \\ 0 & 0 & 0 \end{pmatrix} \begin{Bmatrix} l_1 & l_2 & L \\ L' & n & l'_1 \end{Bmatrix} \\ \left. + (-1)^{l_1+l_2+l'_2+n} \delta_{l_1, l'_1} \sqrt{(2l_2+1)(2l'_2+1)} \right) \\ \times r_2^n \begin{pmatrix} l_2 & n & l'_2 \\ 0 & 0 & 0 \end{pmatrix} \begin{pmatrix} L & n & L' \\ 0 & 0 & 0 \end{pmatrix} \begin{Bmatrix} l_1 & l_2 & L \\ n & L' & l'_2 \end{Bmatrix}. \quad (11)$$

The time-dependent close-coupled equations of equation (7) are propagated separately for the dipole and quadrupole interaction. The coupled radial wavefunctions are then projected onto products of one-electron orbitals to yield scattering probability amplitudes given by

$$\mathcal{P}_{l_1 l_2}^{LS}(k_1, k_2, t) = \int_0^\infty dr_1 \int_0^\infty dr_2 P_{k_1 l_1}(r_1) P_{k_2 l_2}(r_2) P_{l_1 l_2}^{LS}(r_1, r_2, t), \quad (12)$$

where the box normalized continuum orbitals, $P_{kl}(r)$, are calculated in a V^{N-2} potential. The total cross section for double photoionization is given by [7]

$$\sigma = \frac{\omega}{I} \sum_L \frac{\partial}{\partial t} \int_0^\infty dk_1 \int_0^\infty dk_2 \sum_{l_1, l_2} |\mathcal{P}_{l_1 l_2}^{LS}(k_1, k_2, t)|^2, \quad (13)$$

where I is the radiation field intensity. The total integral double photoionization cross section will therefore contain a dipole and a quadrupole term. The single energy differential cross section (SDCS) for double photoionization is given by [7]

$$\frac{d\sigma}{d\alpha} = \frac{\omega}{I} \sum_L \frac{\partial}{\partial t} \int_0^\infty dk_1 \int_0^\infty dk_2 \delta \left(\alpha - \tan^{-1} \left(\frac{k_2}{k_1} \right) \right) \times \sum_{l_1, l_2} |\mathcal{P}_{l_1 l_2}^{LS}(k_1, k_2, t)|^2, \quad (14)$$

where α is the hyperspherical angle. The differential cross section may also be given in terms of the ejected energy:

$$\frac{d\sigma}{dE_1} = \frac{1}{k_1 k_2} \frac{d\sigma}{d\alpha}, \quad (15)$$

where the area under the SDCS corresponds to the total integral cross section. As is clear from equation (14), the SDCS is an incoherent sum containing a pure dipole term and a pure quadrupole term but no dipole–quadrupole interference terms.

The triple differential cross section (TDCS) is given [7] by

$$\frac{d^3\sigma}{d\alpha d\Omega_1 d\Omega_2} = \frac{\omega}{I} \frac{\partial}{\partial t} \int_0^\infty dk_1 \int_0^\infty dk_2 \delta \left(\alpha - \tan^{-1} \left(\frac{k_2}{k_1} \right) \right) \times \left| \sum_L \sum_{l_1, l_2} (-i)^{l_1+l_2} e^{i(\delta_{l_1}+\delta_{l_2})} \mathcal{P}_{l_1 l_2}^{LS}(k_1, k_2, t) Y_{l_1 l_2}^L(\hat{k}_1, \hat{k}_2) \right|^2, \quad (16)$$

where δ_{l_1} and δ_{l_2} are scattered phase shifts and $Y_{l_1 l_2}^L(\hat{k}_1, \hat{k}_2)$ are coupled spherical harmonics. The triple differential cross section is a coherent sum and so in addition to a pure dipole and a pure quadrupole term, a dipole–quadrupole interference term will also be present.

3. Results

Our calculations were made at an incident photon energy of 800 eV. A number of calculations were made to test convergence with respect to the box size, lattice spacing and number of channels. The small magnitude of the double photoionization cross section at a high photon energy of 800 eV makes numerical convergence particularly

Table 1. Channels used in the double photoionization calculations.

Ground state		Dipole		Quadrupole	
l_1	l_2	l_1	l_2	l_1	l_2
0	0	0	1	0	2
1	1	1	0	2	0
2	2	1	2	1	1
3	3	2	1	1	3
4	4	2	3	3	1
5	5	3	2	2	2
6	6	3	4	2	4
7	7	4	3	4	2
8	8	4	5	3	3
9	9	5	4	3	5
10	10	5	6	5	3
11	11	6	5	4	4
12	12	6	7	4	6
		7	6	6	4
		7	8	5	5
		8	7	5	7
		8	9	7	5
		9	8	6	6
		9	10	6	8
		10	9	8	6
		10	11	7	7
		11	10	7	9
		11	12	9	7
		12	11	8	8
		12	13	8	10
		13	12	10	8
				9	9

challenging. Tests were made using a number of lattices, ranging from a 512×512 point lattice with a mesh spacing of $\Delta r = 0.10$ to a 1500×1500 point lattice with a mesh spacing of $\Delta r = 0.05$. The close-coupled equations were propagated for up to 20 radiation field periods. The initial ground state $\Phi_0^S(\mathbf{r}_1, \mathbf{r}_2)$ of the helium atom was found by relaxation of the imaginary time Schrödinger equation using 13 coupled channels for the dipole and 10 coupled channels for the quadrupole calculation. The real-time Schrödinger equation was then solved using 26 $l_1 l_2$ coupled channels for the dipole and 27 $l_1 l_2$ coupled channels for the quadrupole calculation, see table 1 for details.

The results shown are from the largest calculation on the 1500×1500 point lattice. Using the 13 coupled channels shown in table 1, relaxation of the imaginary time Schrödinger equation gave a ground-state energy of -78.80 eV, close to the exact ground state energy of -79.01 [16]. Taking an average over the last five radiation field periods, the total integral cross section for double photoionization due to the dipole interaction was found to be 19.18 b ($1 \text{ b} = 1.0 \times 10^{-24} \text{ cm}^2$) and the total integral cross section due to the quadrupole interaction was found to be 1.21 b. This compares to a total integral double photoionization cross section of 16.9 ± 1.7 b as measured by Samson *et al* [3]. The relatively large contribution of the quadrupole interaction to the total integral double photoionization cross section, with a quadrupole to dipole ratio for the total integral cross section of 6% can be explained by the high photon energy of 800 eV

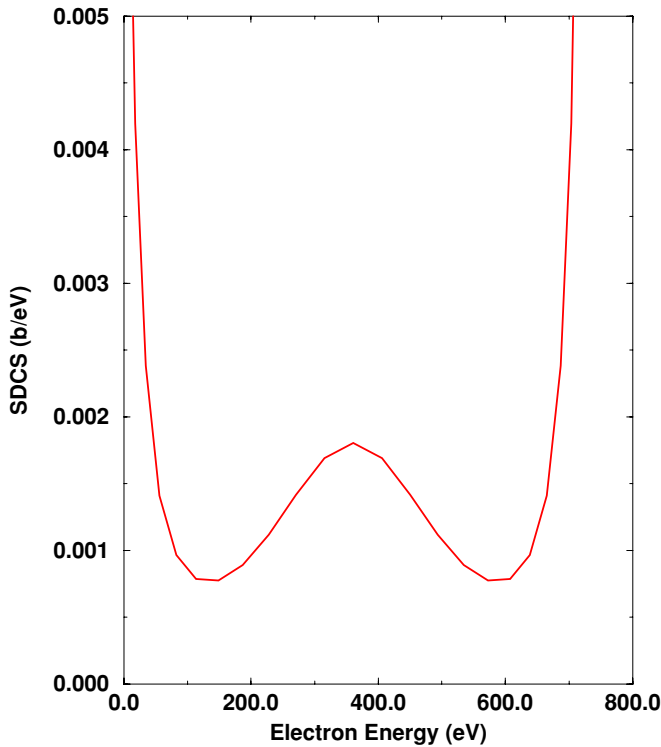


Figure 1. Quadrupole SDCS for double photoionization of helium by an 800 eV photon.

considered, since this enhances the effect of the quadrupole interaction via the $(\frac{\omega}{c})$ term in equation (5).

The quadrupole SDCS for double photoionization is shown in figure 1. The cross section has a ‘W’ shape, with a local maximum at equal energy sharing of the two ejected electrons, thus confirming the model prediction of Amusia [13, 14]. In figure 2, the dipole SDCS is compared to the sum of the dipole and quadrupole SDCSs. The dipole cross section has the characteristic ‘U’ shape observed previously for studies of double photoionization at high photon energies with the ‘shake-off’ mechanism dominating [8]. The addition of the quadrupole SDCS results in only a small shift from the dipole SDCS, so that any planned measurement of the SDCS at this energy will have difficulty in isolating the quadrupole effects. However, at higher photon energies >1 keV the sum of the dipole and quadrupole SDCSs should also develop a pronounced ‘W’ shape as the influence of the quadrupole interaction becomes stronger.

The presence of a local maximum at equal energy sharing in the quadrupole SDCS indicates that non-dipole effects might be enhanced in the triple differential cross section at equal energy sharing. The pure dipole contribution to the TDCS should be zero when the electrons are ejected back to back with equal energy due to the selection rule ‘C’ defined by Maulbetsch and Briggs [17], which states that for $\mathbf{k}_1 = -\mathbf{k}_2$, singlet states with odd parity do not contribute to the cross section. Figure 3 presents the TDCS that contains pure dipole, pure quadrupole and dipole–quadrupole components in comparison to the TDCS containing only the pure dipole component. The TDCSs are at equal energy sharing, $E_1 = E_2$, with co-planar geometry ($\phi_1 = \phi_2 = 0$) and are plotted as a

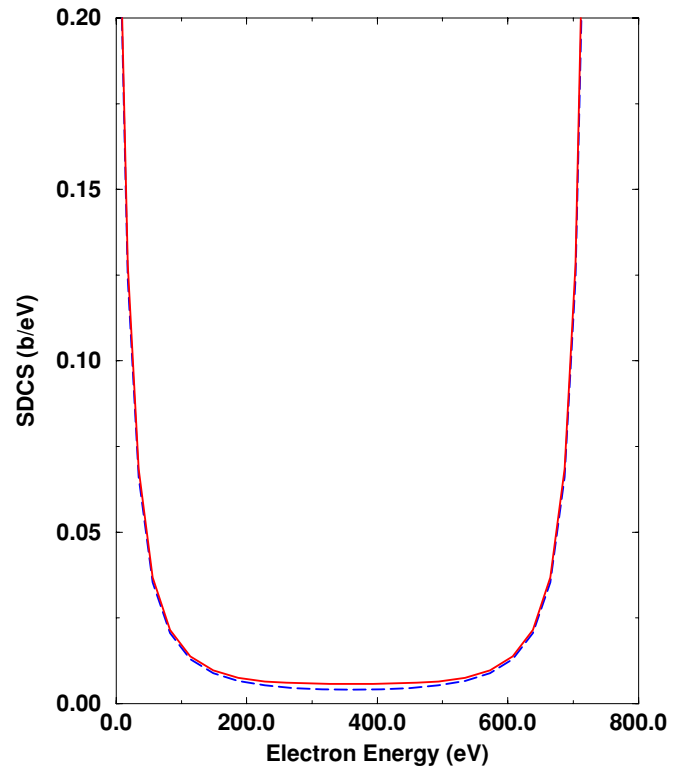


Figure 2. SDCS for double photoionization of helium by an 800 eV photon. Dashed curve: dipole SDCS; solid curve: sum of the dipole and quadrupole SDCSs.

function of θ_2 for $\theta_1 = 0^\circ, 30^\circ, 60^\circ$ and 90° . The angles of the ejected electrons are defined relative to the direction of polarization of the radiation field. Non-dipole effects can be seen most clearly at $\theta_1 = 0^\circ$ and $\theta_1 = 90^\circ$, with the effect of the pure quadrupole component strongest when the ejected electrons are parallel to the polarization direction of the radiation field. The dominant back-to-back feature seen at $(\theta_1 = 0^\circ, \theta_2 = 180^\circ)$ and $(\theta_1 = 90^\circ, \theta_2 = 270^\circ)$ arises entirely from the pure quadrupole component, with the smaller wings arising from the pure dipole component. As experimental resolution improves, this prediction should be amenable to experimental verification as it offers a clear signature of non-dipole effects. Previous work looking at non-dipole effects on the TDCS [9, 10, 12] accounted for the dipole–quadrupole term but neglected the pure quadrupole term and so did not predict this effect.

4. Summary

The inclusion of the quadrupole interaction has been shown to be important in double photoionization of helium at a photon energy of 800 eV, with the quadrupole component of the total integral cross section being 6% the value of the dipole component. The predicted ‘W’ shape of the quadrupole SDCS has been confirmed. Experimental measurements of the summed dipole and quadrupole SDCSs are unlikely to be able to discern non-dipole features at this photon energy due to the small effect and the small cross section magnitude. However, non-dipole features should be clearly visible

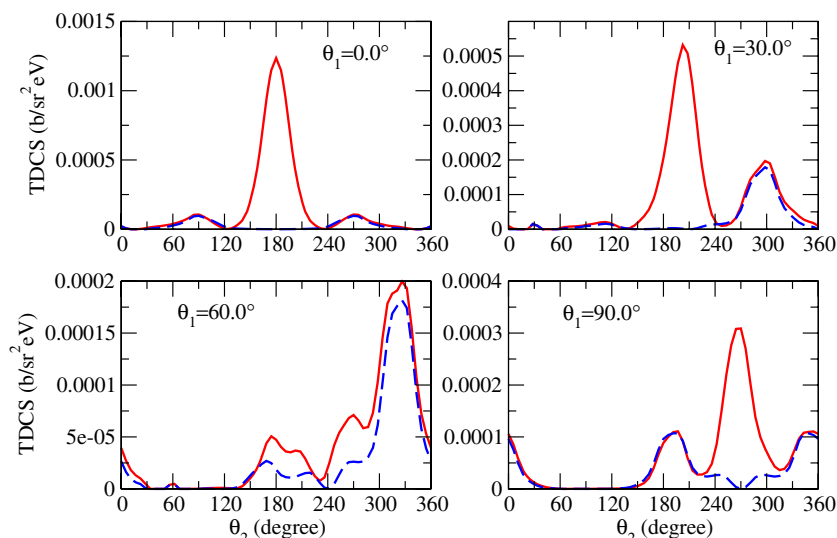


Figure 3. TDCS for double photoionization of helium by an 800 eV photon. The TDCS is plotted at equal energy sharing for $\theta_1 = 0^\circ, 30^\circ, 60^\circ$ and 90° . Dashed curve: TDCS containing only the pure dipole component; solid curve: TDCS containing pure dipole, pure quadrupole and dipole-quadrupole components.

in the TDCS at equal energy sharing, with the pure quadrupole component of the TDCS dominating when the two electrons are ejected back-to-back parallel to the direction of polarization of the radiation field.

Extending the present calculations to higher photon energies would be of great interest as non-dipole effects become progressively more significant. However, numerical convergence issues make such a calculation challenging at the present time. In addition, at higher photon energies, Compton scattering will need to be accounted for. At photon energies >6 keV, double ionization by Compton scattering becomes dominant [18]. We hope that the results presented here will stimulate experimentalists to search for the predicted non-dipole features in the TDCS at equal energy sharing.

Acknowledgments

We would like to thank Alan Landers for suggesting this problem and the referees for helpful suggestions. This work was supported in part by grants from the U.S. Department of Energy and the National Science Foundation. The Los Alamos National Laboratory is operated by Los Alamos National Security, LLC for the National Nuclear Security Administration of the U.S. Department of Energy under Contract No. DE-AC5206NA25396. Computational work was carried out at the National Energy Research Scientific Computing Center in Oakland, CA.

References

- [1] Bräuning H *et al* 1998 *J. Phys. B: At. Mol. Opt. Phys.* **31** 5149
- [2] Knapp A *et al* 2002 *Phys. Rev. Lett.* **89** 033004
- [3] Samson J A R *et al* 1997 *Phys. Rev. A* **57** 1906
- [4] Pindzola M S and Robicheaux F 1998 *Phys. Rev. A* **57** 318
- [5] Kheifets A S and Bray I 1998 *J. Phys. B: At. Mol. Opt. Phys.* **31** L447
- [6] Malegat L, Selles P and Kazansky A K 2000 *Phys. Rev. Lett.* **85** 4450
- [7] Colgan J, Pindzola M S and Robicheaux F 2001 *J. Phys. B: At. Mol. Opt. Phys.* **34** L457
- [8] Colgan J and Pindzola M S 2004 *J. Phys. B: At. Mol. Opt. Phys.* **37** 1153
- [9] Istomin A Y, Manakov N L, Meremianin A V and Starace A F 2004 *Phys. Rev. Lett.* **92** 063002
- [10] Istomin A Y, Manakov N L, Meremianin A V and Starace A F 2005 *Phys. Rev. A* **71** 052702
- [11] Istomin A Y, Starace A F, Manakov N L, Meremianin A V, Kheifets A S and Bray I 2005 *Phys. Rev. A* **72** 052708
- [12] Istomin A Y, Starace A F, Manakov N L, Meremianin A V, Kheifets A S and Bray I 2006 *J. Phys. B: At. Mol. Opt. Phys.* **39** L35
- [13] M Ya Amusia, Drukarev E G, Gorshkov V G and Kazachkov M P 1975 *J. Phys. B: At. Mol. Phys.* **8** 1248
- [14] M Ya Amusia, Drukarev E G and Mandelzweig V B 2005 *Phys. Scr.* **72** C22
- [15] Pindzola M S *et al* 2007 *J. Phys. B: At. Mol. Opt. Phys.* **40** R39
- [16] See <http://physics.nist.gov/PhysRefData>
- [17] Maulbetsch F and Briggs J S 1995 *J. Phys. B: At. Mol. Opt. Phys.* **28** 551
- [18] Dörner R *et al* 2004 *Rad. Phys. Chem.* **70** 191